HHS Public Access

Author manuscript

Mater Sci Eng C Mater Biol Appl. Author manuscript; available in PMC 2023 July 16.

Published in final edited form as:

Mater Sci Eng C Mater Biol Appl. 2020 June ; 111: 110846. doi:10.1016/j.msec.2020.110846.

Impact of composite scaffold degradation rate on neural stem cell persistence in the glioblastoma surgical resection cavity

Kathryn M. Moore[a], **Elizabeth G. Graham-Gurysh**[b], **Hunter N. Bomba**[b], **Ananya B. Murthy**[b], **Eric M. Bachelder**[b], **Shawn D. Hingtgen**[b,c], **Kristy M. Ainslie**[a,b,d,*]

[a]Joint Department of Biomedical Engineering, University of North Carolina at Chapel Hill and North Carolina State University, USA

[b]Division of Pharmacoengineering and Molecular Pharmaceutics, Eshelman School of Pharmacy, University of North Carolina at Chapel Hill, USA

[c]Department of Neurosurgery, UNC School of Medicine, University of North Carolina, Chapel Hill, NC, USA

[d]Department of Microbiology and Immunology, UNC School of Medicine, University of North Carolina, Chapel Hill, NC, USA

Abstract

Tumoricidal neural stem cells (NSCs) are an emerging therapy to combat glioblastoma (GBM). This therapy employs genetically engineered NSCs that secrete tumoricidal agents to seek out and kill tumor foci remaining after GBM surgical resection. Biomaterial scaffolds have previously been utilized to deliver NSCs to the resection cavity. Here, we investigated the impact of scaffold degradation rate on NSC persistence in the brain resection cavity. Composite acetalated dextran (Ace-DEX) gelatin electrospun scaffolds were fabricated with two distinct degradation profiles created by changing the ratio of cyclic to acyclic acetal coverage of Ace-DEX. *In vitro*, fast degrading scaffolds were fully degraded by one week, whereas slow degrading scaffolds had a half-life of > 56 days. The scaffolds also retained distinct degradation profiles *in vivo*. Two different NSC lines readily adhered to and remained viable on Ace-DEX gelatin scaffolds, *in vitro*. Therapeutic NSCs secreting tumor necrosis factor-related apoptosis-inducing ligand (TRAIL) had the same TRAIL output as tissue culture treated polystyrene (TCPS) when seeded on both scaffolds. Furthermore, secreted TRAIL was found to be highly potent against the human derived GBM cell line, GBM8, *in vitro*. Firefly luciferase expressing NSCs were seeded on scaffolds,

*Corresponding author at: Division of Pharmacoengineering and Molecular Pharmaceutics, UNC Eshelman School of Pharmacy, 4211 Marsico Hall, 125 Mason Farm Road, Chapel Hill, NC 27599, USA. ainsliek@email.unc.edu (K.M. Ainslie).

Declaration of competing interest

The authors declare the following financial interests/personal relationships which may be considered as potential competing interests: Drs. Ainslie and Bachelder serve on the advisory board for IMMvention Therapeutix, Inc. Although a financial conflict of interest was identified for management based on the overall scope of the project and its potential benefit to IMMvention Therapeutix, Inc., the research findings included in this publication may not necessarily related to the interests of IMMvention Therapeutix, Inc. Dr. Shawn Hingtgen is the Founder and CSO of Falcon Therapeutics which has exclusively licensed aspects of scaffold-based technology for GBM therapy. The terms of this arrangement have been reviewed and approved by the University of North Carolina at Chapel Hill in accordance with its policy on objectivity in research.

Appendix A. Supplementary data

Supplementary data to this article can be found online at https://doi.org/10.1016/j.msec.2020.110846.

implanted in a surgical resection cavity and their persistence in the brain was monitored by bioluminescent imaging (BLI). NSC loaded scaffolds were compared to a direct injection (DI) of NSCs in suspension, which is the current clinical approach to NSC therapy for GBM. Fast and slow degrading scaffolds enhanced NSC implantation efficiency 2.87 and 3.08-fold over DI, respectively. Interestingly, scaffold degradation profile did not significantly impact NSC persistence. However, persistence and long-term survival of NSCs was significantly greater for both scaffolds compared to DI, with scaffold implanted NSCs still detected by BLI at day 120 in most mice. Overall, these results highlight the benefit of utilizing a scaffold for application of tumoricidal NSC therapy for GBM.

Keywords

Electrospinning; Acetalated dextran; Gelatin; Tumoricidal neural stem cell therapy; TRAIL

1. Introduction

Glioblastoma (GBM) is the most common primary brain tumor and is classified by the World Health Organization (WHO) as Grade IV, the most malignant type of glioma [1]. The current standard of care (surgical resection, oral chemotherapy with temozolomide, and radiation) typically fails to eliminate the tumor, leading to a dismal median patient survival of 15–18 months [2]. There are several contributing factors that limit the efficacy of current GBM therapies, including high tumor infiltration into surrounding tissue, poor drug diffusion in and across the brain, and drug resistance. Moreover, GBM is diffuse and presents invasive projections that prevent gross total surgical resection. While small molecule drugs are limited by various barriers such as short diffusion distances in the tissue and across the blood-brain barrier, stem cells (SCs) may provide therapeutic benefit because they have been shown to migrate throughout the brain and seek out GBM cells in response to chemotactic signals [3,4]. As an emerging strategy to combat GBM, tumoricidal SC therapy employs genetically engineered cells to produce anti-tumor agents so they may seek out and kill remaining tumor cells after resection. SCs can be readily engineered to produce a wide array of therapeutics including tumoricidal proteins, prodrug enzymes, viral vectors, and immunomodulatory molecules [5–7]. Phase I clinical trials have established the safety of injecting tumoricidal SCs in the brain, and Phase II clinical trials are currently underway [8].

Despite their promise, there are considerable challenges remaining for tumoricidal SC therapy for GBM; chiefly, effective and stable implantation of SCs into the surgical resection cavity. Preclinical studies have shown that SCs injected into the GBM surgical resection cavity are cleared rapidly from the brain between 4 and 14 days, whereas SCs seeded on a hyaluronic acid scaffold persist in the brain > 28 days [9]. The increased SC persistence in the brain correlated with enhanced tumor killing and overall survival in mice [9]. The benefit of scaffolds for enhancing persistence of SC after implantation in the resection cavity has been demonstrated using a number of other scaffold types, including those composed of hyaluronic acid (HA), fibrin hydrogels, electrospun poly(L-lactic) acid (PLA), and alginate gels [9–14],[53].

While these results show potential, these prior studies did not characterize the degradation profiles of the scaffolds and as a result, the role of scaffold degradation rate on persistence has yet to be elucidated. This study is aimed at determining the effect of the scaffold degradation profile on neural stem cell (NSC) persistence in the brain, utilizing the novel biomaterial, acetalated dextran (Ace-DEX). Ace-DEX has been used because of its tunable degradation properties to rationally design drug delivery platforms for a variety of therapies [15–18]. By simply changing reaction time, the ratio of cyclic to acyclic acetal coverage (CAC) is altered, which controls the polymer degradation rate that can range from hours to months [19]. Ace-DEX is easily fabricated into scaffolds by electrospinning, a scalable process that generates flexible, fibrous scaffolds [18]. We have previously demonstrated the safety of implanting drug loaded and blank electrospun Ace-DEX scaffolds in the brain [17]. Using Ace-DEX, fast and slow degrading electrospun scaffolds were fabricated, characterized, and evaluated *in vitro* and *in vivo* for their impact on NSC persistence in the brain.

2. Materials and methods

All materials were purchased from Sigma (St. Louis, MO) and used as purchased, unless otherwise indicated.

2.1. Acetalated dextran (Ace-DEX) synthesis

Ace-DEX was synthesized as previously described [20]. Briefly, lyophilized dextran and acid catalyst, pyridinium p-toluenesulfonate (> 98%), were dissolved in anhydrous dimethyl sulfoxide (DMSO, > 99.9%). Under anhydrous conditions, dextran (molecular weight 450–650 kDa) was reacted with 2-ethoxypropene (Matrix Scientific, Columbia, SC) in DMSO for ~16 min or 2 h to generate pendant acetal groups. The reaction was quenched by the addition of triethylamine (TEA, > 99%) and then the mixture was precipitated into basic water and lyophilized. Impurities were removed by dissolving the polymer in ethanol, centrifuging, and precipitating into basic water (0.04% TEA in water). The resulting polymer, Ace-DEX, was lyophilized and stored in −20 °C until further use. Nuclear magnetic resonance (NMR, Varian Inova 400) was used to characterize the relative cyclic acetal coverage (CAC) as previously described [20].

2.2. Ace-DEX gelatin scaffold fabrication

Ace-DEX (75% wt/wt) and gelatin (25% wt/wt) were dissolved in a tri-solvent consisting of hexafluoroisopropanol (> 99%), 1-butanol (≥99.4%), and TEA at a ratio of 89%, 10%, 1% v/v, respectively at a concentration of 150 mg/mL. The polymer solution was pumped out of a glass syringe with a 21-gauge needle at a rate of 2 mL per hour. A voltage bias of 15 kV was applied from the tip of the needle to a collection plate 13 cm apart.

Scaffolds were crosslinked by dehydrothermal (DHT) crosslinking by wrapping in aluminum foil and placing in a vacuum oven at 130 °C under −67.7 kPa for 0–100 h. Then, scaffolds were stored in a vacuum desiccator at room temperature. ICG-loaded Ace-DEX gelatin scaffolds were fabricated as described above, with 0.5% wt/wt ICG (VWR, Randor, PA) added to the polymer solution.

2.3. Scaffold materials characterization

Scaffold morphology was evaluated by scanning electron microscopy (SEM). Scaffolds were mounted onto aluminum stubs using carbon tape. Samples were coated with palladium using a sputter coater and imaged at 2 kV on the Hitachi S-4700 Cold Cathode Field Emission Scanning Electron Microscope. Gelatin loading was determined by fluorescamine assay adapted from a protocol described by Lorenzen et al. using a gelatin standard curve [21]. Non-crosslinked scaffolds were degraded at a concentration of 4 mg/mL in hydrochloric acid (0.1 N), then neutralized by dilution to 1 mg/mL in 0.1 M borate buffer. A fluorescamine assay was performed by combining fluorescamine solution (3 mg/mL in DMSO) with samples at a 1:4 ratio and reading fluorescence in a plate reader (excitation: 390 nm, emission: 460 nm) and comparing to a standard curve.

2.4. In vitro degradation and release studies

Scaffold degradation was measured by mass loss, where pre-weighed scaffolds were placed in individual microcentrifuge tubes containing 1× phosphate buffered saline (PBS, pH 7.4) at 1.5 mg/mL. Tubes were then kept at 37 °C on a shaker plate at 150 RPM. At specific time points, the supernatant was removed and stored at −20 °C for analysis of gelatin release. To determine degradation, scaffolds were washed with basic water (to remove salts from PBS), lyophilized and re-weighed. Mass loss was determined by subtracting final mass from initial mass and normalizing to the initial mass at time 0. The supernatant was tested for gelatin content by a fluorescamine assay [21].

ICG-loaded scaffolds were characterized similarly, where degradation was determined by mass loss at various time points. To determine ICG release, after re-weighing for mass loss, scaffolds were dissolved in DMSO and water (50%:50% v/v). ICG remaining in the scaffolds was evaluated by fluorescence in a plate reader (excitation:788 nm, emission:813 nm) and compared to a standard curve.

2.5. ICG scaffold degradation in vivo

Female athymic nude mice (6–8 weeks of age, University of North Carolina at Chapel Hill Animal Studies Core) were used for all *in vivo* experiments. All experimental protocols were approved by the Animal Care and Use Committees at The University of North Carolina at Chapel Hill.

Scaffold degradation *in vivo* was investigated using a surgical model of resection [10, [9]]. Mice were anesthetized by vapor isoflurane and secured on a three-point stereotaxic apparatus (Stoelting, Kiel, WA). A small circular window in the skull was made using a bone drill (Ideal Microdrill, Harvard Apparatus, Holliston, MA), exposing the right frontal lobe of the brain. A surgical resection cavity approximately 1 mm deep was made by removing a small portion of brain by aspiration. Once bleeding was controlled with the hemostatic agent, Surgicel (Ethicon, Somerville, NJ) and rinsed with cold saline, a single 3 mm ICG-loaded scaffold was implanted (fast, n = 2; slow, n = 2) and the incision was then closed with Vetbond Tissue Adhesive (3 M, Maple-wood, MN). For pain management, meloxicam (5 mg/kg) was administered subcutaneously prior to surgery and then daily for the next 3 days during recovery. Fluorescence from ICG was measured non-invasively in the

brain over time using the Perkin Elmer IVIS Lumina *In Vivo* Imaging System (Waltham, MA) at excitation 710–760 nm and emission 810–875 nm with 1–10 second exposure times. ICG remaining was quantified by normalizing total flux (ρ/s) from each mouse to the total flux from day 0.

2.6. Cell lines

Immortalized C17.2 NSCs were used for initial *in vitro* cell viability experiments. C17.2 s were cultured in Dulbecco's Modified Eagle Medium (DMEM, Corning, Corning, NY) supplemented with 1% penicillin-streptomycin (Hyclone, Pittsburg, PA) and 10% fetal bovine serum (Corning). Primary cortical NSCs derived from CD-1 mice (R&D Systems, Minneapolis, MN) were utilized for *in vitro* GBM killing, TNF-related apoptosis-inducing ligand (TRAIL) output analysis, and *in vivo* experiments. Patient-derived GBM cell line, GBM8, was a kind gift from Dr. Hiroaki Wakimoto (Massachusetts General Hospital, Boston, MA). Primary NSCs and GBM8 cells were cultured in suspension in neuro-basal media (Gibco Laboratories, Gaithersburg, MD) supplemented with 2% B-27 supplement (Gibco Laboratories), 1.5% L-glutamine (Gibco Laboratories), 0.5% N-2 supplement (Gibco Laboratories), 0.5% anti-biotic-antimycotic (Gibco Laboratories), 1 mg heparin (Gibco Laboratories), 10 μg fibroblast growth factor (FGF, Gemini Bio-Products, West Sacramento, CA), and 10 μg epidermal growth factor (EGF, Gemini Bio-Products).

Primary NSCs were transduced by lentivirus encoding either mCherry-firefly luciferase (mCh-FLUC) or GFP-TNF-related apoptosis-inducing ligand (GFP-TRAIL) vectors (Invitrogen, Carisbad, CA). GFP-TRAIL NSCs were isolated by fluorescence-activated cell sorting (FACS). GBM8 cells were transduced with mCh-FLUC, and puromycin selected.

2.7. In vitro NSC seeding and viability on scaffolds

Prior to seeding, 96-well plates were coated with agar (1% wt/v) dissolved in 50% DMEM and 50% PBS. After the agar solidified, scaffolds (punched into 3 mm diameter circles) were placed in the center of the well to hydrate. Slow degrading scaffolds were allowed to hydrate on agar coating overnight, and fast degrading scaffolds required < 0.5 h. Silicone inserts with a 3 mm inner diameter and 5 mm outer diameter were placed on top of each scaffold. Cells were funneled onto scaffolds in 30 μL and allowed to attach for 4 h (Supplemental Fig. 1). Scaffolds were transferred to 0.5 mL media in a 24-well plate 4 h after seeding. In order to get the non-adherent primary NSCs to adhere to the scaffolds, NSCs were first treated with 2% FBS to make them adherent for 24 h in a tissue culture dish before seeding onto scaffolds.

C17.2 cell viability and proliferation were determined by a thiazolyl blue tetrazolium bromide (MTT) assay alongside a cell standard curve in a 24-well plate with 0.5 mL of media. Briefly, cells were incubated with MTT dissolved in media at 0.5 mg/mL for 3 h. Media was then removed, and isopropanol (> 99.5%) was added to dissolve formazan crystals. Absorbance was measured at 560 nm using 670 nm as a reference. Cell seeding efficiency was determined by normalizing number of cells on scaffold at 6 h to number of cells seeded. Cell carrying capacity was calculated by quantifying cell number on scaffolds at 24 h after seeding. Cell viability was measured at 6, 24, and 48 h.

2.8. Quantification of TRAIL output from TRAIL-NSCs on scaffolds

Scaffolds were seeded with TRAIL-NSCs at a density of 2.5×10^5 per well for 4 h, and then were transferred into a 96 well plate with 200 μL of media. At the same time, a range of cell densities were also seeded on TCPS in a 96-well plate with 200 μL of media. Twenty-four hours after seeding, the media was replaced with fresh and allowed to be conditioned by the cells in the incubator for 4 h. Media was then collected and stored in −20 °C for TRAIL quantification by human TRAIL ELISA kit (Invitrogen). Cells were dissociated from scaffolds or the 96-well plate and counted by hemocytometer. TRAIL output was normalized by cell number.

2.9. In vitro GBM killing

A co-culture experiment was performed in a 96-well plate by seeding a fixed number of mCherry-FLUC-GBM8 tumor cells (1×10^4 per well) along with a range of TRAIL-NSCs or NSCs (blank) (1.25×10^3–4×10^4 cells per well) in a total of 200 μL of media. After 72 h of co-culture, GBM8 viability was determined by bioluminescence using a plate reader (BioTek Instruments, Winooski, VT) and normalized to untreated GBM8 cells.

TRAIL-conditioned media was generated after 6.5 h of TRAIL-NSC (2.5×10^5 per well) incubation in a 96-well plate. TRAIL concentration in the conditioned media was quantified by ELISA. GBM8 tumor cells (2×10^4 per well) were treated for 48 h with serially diluted TRAIL-conditioned media in a 96-well plate with a total of 200 μL of media. GBM8 viability was measured by MTT assay to calculate the half maximal inhibitory concentration (IC_{50}) of TRAIL secreted by NSCs.

2.10. NSC persistence model

The effect of scaffolds on NSC persistence was evaluated in the surgical model described above. 2.5×10^5 mCherry-FLUC-NSCs were implanted in the resection cavity either seeded onto a single 3 mm scaffold or by direct injection (DI) loaded into a Hamilton syringe in 4 μL PBS (fast, n = 5; slow, n = 4; DI = 5). NSC persistence was monitored by bioluminescent imaging (BLI) for the duration of the study (120 days). At each imaging time point, mice were anesthetized by inhaled isoflurane and imaged by the Perkin Elmer IVIS Lumina *In Vivo* Imaging System. Mice were given an intraperitoneal injection of D-luciferin (15 mg/kg in PBS; Perkin Elmer) and imaged 25 min later at a 5 minute exposure to monitor NSC persistence. Image exposure length and time after D-luciferin injection was optimized to maximize BLI signal. BLI signal (total flux, ρ/s) was normalized to background signal from a mouse containing no NSCs. NSC implant efficacy was determined by quantifying the BLI signal from each mouse on day 2 and normalizing it to the “maximum intended dose” which is the average BLI signal from the 5 mice with the highest signal, regardless of group. The time to NSC clearance was determined by fitting trendlines to the normalized BLI signal for each mouse and applying a threshold of 15% of “maximum intended dose” (Supplemental Fig. 2). The time to clearance was plotted as a Kaplan-Meier survival curve.

2.11. Statistical analysis

Statistical analysis was performed using GraphPad Prism (La Jolla, CA). Cell seeding and growth comparisons were performed by Student *t*-test. Kaplan-Meier curves of NSC

clearance in the brain were analyzed by Log-Rank (Mantel-Cox) test. All other comparisons done by one-way ANOVA with Tukey's Multiple Comparisons post-test.

3. Results and discussion

3.1. Fabricating Ace-DEX gelatin scaffolds by electrospinning and dehydrothermal crosslinking

In tissue engineering, degradation has been regarded as an important scaffold parameter, where it is widely accepted that the rate of scaffold degradation should match the rate of tissue formation to allow for smooth integration into the surrounding tissue [23]. However in NSC-based cancer therapy, the goal is to stabilize transplanted cells post-surgery, then ultimately release the therapeutic cells into brain where they can track down residual cancer foci. By investigating the role of scaffold degradation, we could move towards a more optimal NSC therapy for GBM. Previously, scaffold degradation has been tuned by blending differently degrading polymers [24,25] and changing fabrication parameters that include polymer concentration [26], solvent properties [27], and crosslinking [28]. Here, we utilized the tunability of Ace-DEX to generate scaffolds with two different degradation times. Reacting Ace-DEX for approximately 16 min or 2 h resulted in polymer with an average of 46.0 ± 0.7 or 61.3% ± 1.7 CAC, respectively (Fig. 1A). These times were chosen based on previous studies to generate "fast" and "slow" degrading polymers [29]. Initially, it was determined that NSCs would not attach to pure Ace-DEX electrospun scaffolds, likely due to the hydrophobicity of the polymer (data not shown). In order to facilitate NSC adherence, Ace-DEX polymer was blended with gelatin, a widely used, natural biopolymer derived from denatured collagen [28,30,31]. Furthermore, a commercially available gelatin foam named Gelfoam® has been utilized for hemostasis during brain surgery, illustrating the safety of gelatin for use in the brain [32]. With the addition of gelatin, we anticipated that NSCs would readily adhere to the scaffolds, consistent with previous reports in the literature [33–35].

Composite scaffolds were fabricated with a gelatin mass loading of 28.4% ± 1.97 and 29.0% ± 1.65 for fast and slow scaffolds, respectively (Fig. 1A). Next, scaffolds were stabilized *via* dehydrothermal (DHT) crosslinking to prevent rapid release of hydrophilic gelatin when placed in aqueous solution. Under high heat and vacuum, amide bonds are generated by condensation reactions between adjacent amino acid residues resulting in crosslinked gelatin [36,37]. DHT crosslinking was utilized because it does not pose the potential risk of toxicity that can be seen with more commonly used chemical crosslinkers like glutar-aldehyde [28]. Scaffolds were crosslinked for times ranging from 0 to 112 h and then evaluated for gelatin release (Supplemental Fig. 3A–B). Un-crosslinked scaffolds rapidly released gelatin upon incubation in PBS and had released almost all gelatin within 72 h. However, with increasing DHT crosslinking time, the rate of gelatin release decreased. Saturation of gelatin crosslinking was achieved by increasing DHT time until the gelatin release profile plateaued, occurring between 99 and 112 h for both scaffolds (Supplemental Fig. 3A–B). For this reason, 100 h was chosen as the crosslinking time for the remainder of the study. Scanning electron microscopy (SEM) micrographs demonstrate that scaffold morphology was not altered after 100 h of DHT crosslinking (Supplemental Fig. 3C–F).

The effect of DHT time on crosslinking has been previous reported, however, with different results likely due to scaffold composition. Haugh et al. found that DHT times beyond 24 h resulted in no further crosslinking of freeze dried collagen scaffolds [36]. This is in line with our results which indicate a saturation of crosslinking occurs; however, these pure collagen scaffolds may achieve crosslinking saturation more rapidly compared to our composite scaffolds, where the presence of Ace-DEX may increase the distance between amino acid residues on gelatin.

3.2. Degradation of Ace-DEX gelatin scaffolds in vitro and in vivo

Despite blending with gelatin, the influence of Ace-DEX cyclic acetal coverage (CAC) remained the driver of scaffold degradation, *in vitro*. Ace-DEX gelatin scaffolds composed of polymer with 46.0% ± 0.7 CAC degraded rapidly, with only 25% mass remaining by day three (Fig. 1A–B). Conversely, scaffolds composed of the 61.3% ± 1.7 CAC Ace-DEX had ~60% mass was remaining on day 56. After an initial burst release of gelatin within the first 24 h, the remaining scaffold mass attributed to gelatin was relatively stable over time. This is likely due to saturation of gelatin crosslinking by DHT. SEM micrographs show that Ace-DEX CAC does not influence scaffold morphology (Fig. 1D–E).

In order to investigate Ace-DEX gelatin scaffold degradation *in vivo*, indocyanine green (ICG), a near infrared fluorescent dye, was added to the composite scaffolds. ICG loaded composite scaffolds had the same degradation rate as un-loaded blank composite scaffolds (data not shown). Because ICG is embedded in the scaffold fibers and not chemically conjugated, its release from the scaffolds is likely governed by a combination of diffusion and polymer degradation [38]. While the ICG release from fast degrading scaffold tightly follows its degradation profile *in vitro*, the slow degrading scaffold releases ICG more rapidly than it degrades (Fig. 2A). Yet, the fast and slow degrading scaffolds exhibit unique ICG release rates allowing us to approximate scaffold degradation *in vivo*. *In vivo*, ICG fluorescence was monitored non-invasively using serial fluorescent imaging after being implanted in the brain resection cavity. Interestingly, mice bearing fast degrading scaffolds had 2% of their original fluorescent signal after 7 days compared to 18% at the same timepoint *in vitro*, suggesting that their degradation profile *in vivo* is slower than *in vitro* (Fig. 2B–C). On day 28, there was < 0.15% of the initial fluorescent signal from the fast degrading scaffold group compared to the slow degrading scaffold group which had on average a signal 6.72× higher signal (Fig. 2B). Consistent with our *in vitro* study, these results illustrate a difference in degradation between the fast and slow Ace-DEX gelatin scaffolds *in vivo*.

Scaffold degradation has been found to impact brain tissue regeneration after CNS injury [26,39,40]. Ghuman et al. generated hydrogels that degraded in the brain at rates similar to Ace-DEX gelatin scaffolds by changing protein concentration [26]. This work showed that degradation influenced neural tissue regeneration, with the rapidly degrading hydrogel leading to neovascularization and an increase in infiltrative cells such as neurons and oligodendrocytes in the stroke cavity. Considering the significant influence of scaffold degradation on the local microenvironment after CNS injury, we investigated how scaffold

degradation would affect the persistence of NSCs implanted in the surgical resection cavity with Ace-DEX gelatin scaffolds of two distinct degradation rates.

3.3. Effect of Ace-DEX gelatin scaffold degradation on NSCs in vitro and in vivo

For clinical translation, controlling the number of implanted cells is important for standardizing patient dose. Therefore, we evaluated the ability of the Ace-DEX gelatin scaffolds to hold a high capacity of NSC while maintaining viability. A series of *in vitro* studies were performed with an immortalized murine NSC line, C17.2, for initial scaffold testing. The NSC carrying capacity and seeding efficacy was measured on scaffolds scaled to fit in the surgical resection cavity of the murine brain (Fig. 3A). With increasing number of cells, the seeding efficiency decreased slowly until the number of cells adhered to the scaffolds at 24 h approached a saturation of 139,000 ± 15,700 cells and 114,000 ± 14,900 per a 3 mm scaffold for fast and slow degrading scaffolds, respectively, when 500,000 cells were seeded (Fig. 3B). There was no statistical significance between fast and slow degrading scaffolds for cell carrying capacity or seeding efficiency (Fig. 3C). Previous studies using electrospun scaffolds have only reported the cell number seeded, which may not be the accurate number of cells that adhere to the scaffolds are subsequently implanted in the brain [10].

Moving forward to *in vivo* studies, a primary murine cortical NSC line was utilized, as the immortalized line C17.2 was found to pro-liferate rapidly when implanted in the brains of nude mice (data not shown). Primary NSCs were able to be seeded onto the scaffolds at a higher seeding efficiency than immortalized cells, where the maximum number of cells was 190,000 ± 69,800 cells on fast and 165,000 ± 40,300 cells on slow degrading scaffolds when seeding 250,000 cells (Fig. 3C). We hypothesize this increase in seeding efficiency is because the primary NSC are smaller than the immortalized line. Similar to the immortalized NSC line, primary NSCs maintained the same level of viability after seeding onto scaffolds and supported proliferation for 48 h (Fig. 3D). Despite the fact that fast degrading Ace-DEX gelatin scaffolds had only 32% mass remaining by 48 h, NSC remain viable (Figs. 1C, 3D). This is in line with literature, where Hackett et al. found that 72 h after seeding, around 90% of NSCs remained viable on electrospun composite polycaprolactone collagen scaffolds despite the scaffold degrading completely by 100 h [41]. These results support our finding that NSCs can maintain viability despite significant scaffold degradation.

In addition to the number of cells implanted, the amount of therapy released from the cells is vital to characterize. TRAIL was selected for its potency against GBM, which induces apoptosis *via* binding to the death receptor 5 on the surface of cancer cells, and because it is commonly used in tumoricidal SC studies [42–44]. NSCs transduced with a lenti-viral vector for TRAIL have been previously reported [44–46], and a similar method was used here. To investigate if Ace-DEX gelatin scaffolds would alter therapeutic efficacy, TRAIL output was measured from TRAIL-NSCs seeded onto scaffolds and TCPS. Our results indicate that TRAIL output per cell was the same across both fast (3.20 ± 1.20 fg/cell) and slow (3.23 ± 1.13 fg/cell) degrading scaffolds as well as TCPS (2.81 ± 0.665 fg/cell), suggesting that the nanofibrous structure does not alter TRAIL secretion (Fig. 4A). In

addition, we determined that TRAIL output was not affected by NSC density and correlated linearly with NSC number (Supplemental Fig. 4).

To evaluate the efficacy of secreted TRAIL, TRAIL-NSCs were cultured in the presence of a human derived GBM cell line, GBM8. TRAIL-NSCs showed potent killing compared to control unmodified NSCs (Fig. 4B). In order to investigate the amount of TRAIL required to kill GBM cells *in vitro*, GBM cells were treated for 48 h with supernatant conditioned by TRAIL-NSCs (Fig. 4C). The half maximal inhibitory concentration (IC_{50}) of GBM8 cells was determined to be 8.63 ng TRAIL/mL. Taken together, these studies suggest that TRAIL-NSCs seeded onto Ace-DEX gelatin scaffolds should be highly effective in killing GBM *in vivo*.

In order to determine the impact of scaffold degradation on NSC persistence, a murine model of surgical resection was utilized to recapitulate implantation of the NSCs after debulking a GBM tumor, and thus maintain clinical relevance. Firefly luciferase expressing NSCs were seeded onto scaffolds for 24 h and then implanted into a surgical resection cavity in the right frontal lobe of nude mice. NSCs on scaffolds were compared to a direct injection (DI) of an equivalent number of cells into the wall of the resection cavity, mimicking the current administration of therapeutic NSCs in the clinic [47]. BLI was used to monitor NSC persistence over time (Fig. 5A). Both fast and slow degrading Ace-DEX gelatin scaffolds increased the delivery efficacy of NSCs into the resection cavity 2.87 and 3.08-fold, respectively, (P-value = 0.0047, P-value = 0.0034) over DI (Fig. 5B). Bagó et al. saw a similar increase in SC delivery efficacy by fibrin scaffolds compared to DI, reporting a 2.17-fold increase in human mesenchymal stem cell (MSC) BLI signal at 3 h after implantation [11]. Additionally, Hansen et al. reported increased NSC delivery efficacy using an ECM-based scaffold compared to DI as measured by number of NSC that migrated from the resection cavity to an established GBM tumor in the con-tralateral hemisphere 1 week after implantation [48]. The prevailing hypothesis in the literature for scaffold enhanced transplant efficacy is that providing SCs with a substrate for attachment during the implantation process prevents mechanical wash-out from the resection cavity by cerebrospinal fluid and reduction in programmed cell death [14,48].

Fast and slow degrading scaffolds also had a significantly increased area under the curve (AUC) for BLI signal compared to DI (Fig. 5C, P-value = 0.0107 and P-value = 0.0037, respectively). Furthermore, both fast and slow degrading Ace-DEX gelatin scaffolds significantly extend the length of time that NSCs persist in the brain compared to the DI, P-value = 0.0039 and P-value = 0.0472, respectively (Fig. 5D). The time to NSC clearance below the 15% BLI threshold is longer for the slow degrading scaffold group compared to fast, however not significantly (P-value = 0.0766), with a median persistence of 21 *versus* 16 days (Fig. 5D). Our results demonstrate that scaffolds enhance SC persistence in the surgical resection cavity over DI which has been seen previously with other SC lines [[9],10,11,49,51[53]]. Other previous studies with scaffolds compared persistence of SCs implanted into the brain surgical resection cavity with DI also *via* BLI signal, yet only monitor persistence until 28 days at the latest [9–11]. Bagó et al. found that fibrin scaffolds extended persistence of human MSCs implanted into a resection cavity in the brain > 14 days compared to DI in the resection cavity [11]. The BLI signal for SC implanted

by DI, normalized to its initial signal on day 0, was non-existent by day 14, as well as representative images showing disappearance in pixels attributed to BLI signal between day 10 and 14 as well. In the same time frame, Kauer et al. reported that murine NSCs administered by DI cleared between 7 and 14 days [9]. These results are in line with ours, where all mice that received NSCs administered by DI had cleared by day 11 determined by our threshold (Fig. 5D). Hansen et al. observed a longer persistence of NSCs, reporting that NSCs were still detectable by histology at day 36 [48]. However, the disparity in persistence seen there could be due to the difference in sensitivity of NSC detection method.

Interestingly, Ace-DEX gelatin scaffolds extend long-term survival of NSCs in the brain significantly compared to DI. NSC BLI signal still detected in both scaffold groups at day 120, despite *in vitro* degradation occurring within ~7 days and ICG having only 0.15% of its original fluorescent signal after 28 days (Figs. 1C, 2B, 5A). Yan et al. utilized a composite scaffold, composed the polysaccharide, chitosan, and collagen to transplant MSCs after traumatic brain injury. They found that MSCs seeded on the scaffolds incurred a greater cognitive improvement compared to MSCs administered by DI. The scaffolds had degraded by 1 month after implantation and MSCs transplanted on the scaffolds had differentiated into neurons or glial cells, suggesting that a relatively rapidly degrading scaffold is sufficient to enhance MSC persistence [51].

While there was a trend towards more NSCs remaining in the brain with slower scaffold degradation rates in our study, this was not statistically significant compared to fast scaffolds. One explanation for the minimal difference in NSC persistence may be that increasing NSC implant efficacy is the main factor influencing NSC survival in the brain. Moreover, the NSCs may also be remodeling the fast degrading scaffolds with ECM, allowing them to sustain viability in the cavity beyond the lifetime of the original scaffold [52]. Overall, the results of this study support literature findings that the use of a scaffold increases short-term and long-term persistence of NSCs in the brain. As such, we conclude that scaffold degradation in the time range we explored has a limited impact on the persistence of NSCs in the resection cavity.

4. Conclusion

Tumoricidal SC therapy is a promising avenue for GBM therapy due to the ability to overcome conventional drug delivery barriers. While scaffolds have been found to improve SC implantation in the resection cavity, the role of scaffold degradation rate on SC persistence has not been investigated systematically. To this end, the tunability of the Ace-DEX polymer platform allowed us to generate composite scaffolds with two different degradation profiles *in vitro* and *in vivo* simply by changing the reaction time of Ace-DEX polymer synthesis. *In vitro*, fast degrading scaffolds degraded within 7 days while slow degrading scaffolds retained 60% of its mass out to 56 days. Scaffold degradation did not influence NSC seeding efficiency, short-term viability, or TRAIL output *in vitro*. The effect of scaffold degradation was evaluated in a clinically relevant orthotopic mouse model that mimics surgical GBM resection. Ace-DEX gelatin scaffolds significantly increased NSC implantation efficacy and long-term persistence compared to DI. However, scaffold degradation profile had limited impact on NSC persistence. These results illustrate the

importance of supporting NSCs during the process of implantation to enhance NSC persistence in the brain after surgical resection.

Supplementary Material

Refer to Web version on PubMed Central for supplementary material.

Acknowledgements

This work was supported by the National Institutes of Health (R01NS097507-02, F32CA225199) and National Science Foundation Graduate Research Fellowship Program (NSF-GRFP; DGE-1650116). We would like to thank the Chapel Hill Analytical and Nanofabrication Laboratory (CHANL) for SEM instrumentation, the Biomedical Research Imaging Core (BRIC) for IVIS instrumentation, and the Eshelman School of Pharmacy's NMR Core.

References

[1]. Kanu OO, Mehta A, Di C, Lin N, Bortoff K, Bigner DD, Yan H, Adamson DC, Glioblastoma Multiforme: A Review of Therapeutic Targets, http://dxdoiorg/101517/14728220902942348.

[2]. Lieberman F, Glioblastoma update: molecular biology, diagnosis, treatment, response assessment, and translational clinical trials, F1000Res 6 (2017) 1892 Epub 2017/12/22 10.12688/f1000research.11493.1. [PubMed: 29263783]

[3]. Aboody KS, Brown A, Rainov NG, Bower KA, Liu S, Yang W, Small JE, Herrlinger U, Ourednik V, Black PM, Breakefield XO, Snyder EY, Neural stem cells display extensive tropism for pathology in adult brain: evidence from intracranial gliomas, Proc. Natl. Acad. Sci. U. S. A 97 (23) (2000) 12846–12851 Epub 2000/11/09 10.1073/pnas.97.23.12846. [PubMed: 11070094]

[4]. Tang Y, Shah K, Messerli SM, Snyder E, Breakefield X, Weissleder R, In vivo tracking of neural progenitor cell migration to glioblastomas, Hum. Gene Ther 14 (13) (2003) 1247–1254 Epub 2003/09/04 10.1089/104303403767740786. [PubMed: 12952596]

[5]. Stuckey DW, Shah K, Stem cell-based therapies for cancer treatment: separating hope from hype, Nat. Rev. Cancer 14 (10) (2014) 683–691, 10.1038/nrc3798 [PubMed: 25176333]

[6]. Shah K, Hingtgen S, Kasmieh R, Figueiredo JL, Garcia-Garcia E, Martinez-Serrano A, Breakefield X, Weissleder R, Bimodal viral vectors and in vivo imaging reveal the fate of human neural stem cells in experimental glioma model, J. Neurosci 28 (17) (2008) 4406–4413, 10.1523/JNEUROSCI.0296-08.2008 [PubMed: 18434519]

[7]. Lopez-Ornelas A, Vergara P, Segovia J, Neural stem cells producing an inducible and soluble form of Gas1 target and inhibit intracranial glioma growth, Cytotherapy 16 (7) (2014) 1011–1023 Epub 2014/02/18 10.1016/j.jcyt.2013.12.004. [PubMed: 24529556]

[8]. Portnow J, Synold TW, Badie B, Tirughana R, Lacey SF, D'Apuzzo M, Metz MZ, Najbauer J, Bedell V, Vo T, Gutova M, Frankel P, Chen M, Aboody KS, Neural stem cell-based anticancer gene therapy: a first-in-human study in recurrent high-grade glioma patients, Clin. Cancer Re 23 (12) (2017) 2951–2960 Epub 2016/12/17 10.1158/1078-0432.ccr-16-1518.

[9]. Kauer TM, Figueiredo JL, Hingtgen S, Shah K, Encapsulated therapeutic stem cells implanted in the tumor resection cavity induce cell death in gliomas, Nat. Neurosci 15 (2) (2011) 197–204, 10.1038/nn.3019 [PubMed: 22197831]

[10]. Bago JR, Pegna GJ, Okolie O, Mohiti-Asli M, Loboa EG, Hingtgen SD, Electrospun nanofibrous scaffolds increase the efficacy of stem cell-mediated therapy of surgically resected glioblastoma, Biomaterials 90 (2016) 116–125, 10.1016/j.biomaterials.2016.03.008 [PubMed: 27016620]

[11]. Bago JR, Pegna GJ, Okolie O, Hingtgen SD, Fibrin matrices enhance the transplant and efficacy of cytotoxic stem cell therapy for post-surgical cancer, Biomaterials 84 (2016) 42–53, 10.1016/j.biomaterials.2016.01.007 [PubMed: 26803410]

[12]. Farrell K, Joshi J, Kothapalli CR, Injectable uncrosslinked biomimetic hydrogels as candidate scaffolds for neural stem cell delivery, J. Biomed. Mater. Res. A 105 (3) (2017) 790–805 Epub 2016/11/01 10.1002/jbm.a.35956. [PubMed: 27798959]

[13]. Compte M, Cuesta AM, Sanchez-Martin D, Alonso-Camino V, Vicario JL, Sanz L, Alvarez-Vallina L, Tumor immunotherapy using gene-modified human mesenchymal stem cells loaded into synthetic extracellular matrix scaffolds, Stem Cells 27 (3) (2009) 753–760 Epub 2008/12/20 10.1634/stemcells.2008-0831. [PubMed: 19096041]

[14]. Shafiq M, Jung Y, Kim SH, Insight on stem cell preconditioning and instructive biomaterials to enhance cell adhesion, retention, and engraftment for tissue repair, Biomaterials. 90 (2016) 85–115 Epub 2016/03/27 10.1016/j.biomaterials.2016.03.020. [PubMed: 27016619]

[15]. Collier MA, Gallovic MD, Bachelder EM, Sykes CD, Kashuba A, Ainslie KM, Saquinavir loaded acetalated dextran microconfetti – a long acting protease inhibitor injectable, Pharm. Res 33 (8) (2016) 1998–2009, 10.1007/s11095-016-1936-y [PubMed: 27154460]

[16]. Bachelder EM, Pino EN, Ainslie KM, Acetalated dextran: a tunable and acid-labile biopolymer with facile synthesis and a range of applications, (2016), 10.1021/acs.chemrev.6b00532.

[17]. Graham-Gurysh E, Moore KM, Satterlee AB, Sheets KT, Lin FC, Bachelder EM, Miller CR, Hingtgen SD, Ainslie KM, Sustained delivery of doxorubicin via acetalated dextran scaffold prevents glioblastoma recurrence after surgical resection, Mol. Pharm 15 (3) (2018) 1309–1318 Epub 2018/01/18 10.1021/acs.molpharmaceut.7b01114. [PubMed: 29342360]

[18]. Borteh HM, Gallovic MD, Sharma S, Peine KJ, Miao S, Brackman DJ, Gregg K, Xu Y, Guo X, Guan J, Bachelder EM, Ainslie KM, Electrospun acetalated dextran scaffolds for temporal release of therapeutics, Langmuir 29 (25) (2013) 7957–7965, 10.1021/la400541e [PubMed: 23725054]

[19]. Kauffman KJ, Do C, Sharma S, Gallovic MD, Bachelder EM, Ainslie KM, Synthesis and characterization of acetalated dextran polymer and microparticles with ethanol as a degradation product, ACS Appl. Mater. Interfaces 4 (8) (2012) 4149–4155 Epub 2012/07/27 10.1021/am3008888. [PubMed: 22833690]

[20]. Bachelder EM, Beaudette TT, Broaders KE, Dashe J, Fréchet JMJ, Acetal-derivatized dextran: an acid-responsive biodegradable material for therapeutic applications, J. Am. Chem. Soc 130 (32) (2008) 10494–10495, 10.1021/ja803947s. [PubMed: 18630909]

[21]. Lorenzen A, Kennedy SW, A fluorescence-based protein assay for use with a mi-croplate reader, Anal. Biochem 214 (1) (1993) 346–348 Epub 1993/10/01 10.1006/abio.1993.1504. [PubMed: 8250247]

[23]. Lins LC, Wianny F, Livi S, Hidalgo IA, Dehay C, Duchet-Rumeau J, Gerard JF, Development of bioresorbable hydrophilic-hydrophobic electrospun scaffolds for neural tissue engineering, Biomacromolecules 17 (10) (2016) 3172–3187 Epub 2016/09/16 10.1021/acs.biomac.6b00820. [PubMed: 27629596]

[24]. Kim K, Yu M, Zong X, Chiu J, Fang D, Seo YS, Hsiao BS, Chu B, Hadjiargyrou M, Control of degradation rate and hydrophilicity in electrospun non-woven poly(D,L-lactide) nanofiber scaffolds for biomedical applications, Biomaterials 24 (27) (2003) 4977–4985 Epub 2003/10/16 10.1016/s0142-9612(03)00407-1. [PubMed: 14559011]

[25]. Zhou X, Pan Y, Liu R, Luo X, Zeng X, Zhi D, Li J, Cheng Q, Huang Z, Zhang H, Wang K, Biocompatibility and biodegradation properties of polycaprolactone/polydioxanone composite scaffolds prepared by blend or co-electrospinning, https://doiorg/101177/0883911519835569 (2019), 10.1177/0883911519835569.

[26]. Ghuman H, Mauney C, Donnelly J, Massensini AR, Badylak SF, Modo M, Biodegradation of ECM hydrogel promotes endogenous brain tissue restoration in a rat model of stroke, Acta Biomater. 80 (2018) 66–84 Epub 2018/09/21 10.1016/j.actbio.2018.09.020. [PubMed: 30232030]

[27]. Wang Y, Rudym DD, Walsh A, Abrahamsen L, Kim HJ, Kim HS, Kirker-Head C, Kaplan DL, In vivo degradation of three-dimensional silk fibroin scaffolds, Biomaterials 29 (24–25) (2008) 3415–3428 Epub 2008/05/27 10.1016/j.biomaterials.2008.05.002. [PubMed: 18502501]

[28]. Yang G, Xiao Z, Long H, Ma K, Zhang J, Ren X, Zhang J, Assessment of the characteristics and biocompatibility of gelatin sponge scaffolds prepared by various crosslinking methods, Sci. Rep 8 (1) (2018) 1–13, 10.1038/s41598-018-20006-y. [PubMed: 29311619]

[29]. Chen N, Collier MA, Gallovic MD, Collins GC, Sanchez CC, Fernandes EQ, Bachelder EM, Ainslie KM, Degradation of acetalated dextran can be broadly tuned based on cyclic acetal coverage and molecular weight, Int. J. Pharm 512 (1) (2016) 147–157 Epub 2016/08/21 10.1016/j.ijpharm.2016.08.031. [PubMed: 27543351]

[30]. Echave MC, Saenz del Burgo L, edraz JL, Orive G, Gelatin as biomaterial for tissue engineering, Curr. Pharm. Des 23 (24) (2017) 3567–3584 Epub 2017/05/13 10.2174/1381612823666170511123101. [PubMed: 28494717]

[31]. Afewerki S, Sheikhi A, Kannan S, Ahadian S, Khademhosseini A, Gelatin-polysaccharide composite scaffolds for 3D cell culture and tissue engineering: towards natural therapeutics, Bioeng. Transl. Med 4 (1) (2019) 96–115 Epub 2019/01/27 10.1002/btm2.10124. [PubMed: 30680322]

[32]. Liu X, Ma PX, Phase separation, pore structure, and properties of nanofibrous gelatin scaffolds, Biomaterials 30 (25) (2009) 4094–4103 Epub 2009/06/02 10.1016/j.biomaterials.2009.04.024. [PubMed: 19481080]

[33]. Hutson CB, Nichol JW, Aubin H, Bae H, Yamanlar S, Al-Haque S, Koshy ST, Khademhosseini A, Synthesis and Characterization of Tunable Poly(Ethylene Glycol): Gelatin Methacrylate Composite Hydrogels, https://homeliebertpubcom/tea.

[34]. ZX M, YS W, Z. W M C, Z. YF L L, Electrospinning of PLGA/gelatin randomly-oriented and aligned nanofibers as potential scaffold in tissue engineering, Mater. Sci. Eng (2010) 1204–1210.

[35]. Liu S, Sun X, Wang T, Chen S, Zeng CG, Xie G, Zhu Q, Liu X, Quan D, Nano-fibrous and ladder-like multi-channel nerve conduits: degradation and modification by gelatin, Mater. Sci. Eng. C Mater. Biol. Appl 83 (2018) 130–142 Epub 2017/12/07 10.1016/j.msec.2017.11.020. [PubMed: 29208270]

[36]. Haugh MG, Jaasma MJ, O'Brien FJ, The effect of dehydrothermal treatment on the mechanical and structural properties of collagen-GAG scaffolds, J. Biomed. Mater. Res. A 89 (2) (2009) 363–369 Epub 2008/04/24 10.1002/jbm.a.31955. [PubMed: 18431763]

[37]. Drexler JW, Powell HM, Dehydrothermal crosslinking of electrospun collagen, Tissue Eng. Part C Methods 17 (1) (2011) 9–17, 10.1089/ten.TEC.2009.0754. [PubMed: 20594112]

[38]. Chou SF, Carson D, Woodrow KA, Current strategies for sustaining drug release from electrospun nanofibers, J. Control. Release 220 (Pt B) (2015) 584–591, 10.1016/j.jconrel.2015.09.008. [PubMed: 26363300]

[39]. Wong DY, Hollister SJ, Krebsbach PH, Nosrat C, Poly(epsilon-caprolactone) and poly (L-lactic-co-glycolic acid) degradable polymer sponges attenuate astrocyte response and lesion growth in acute traumatic brain injury, Tissue Eng. 13 (10) (2007) 2515–2523 Epub 2007/07/28 10.1089/ten.2006.0440. [PubMed: 17655492]

[40]. Wang Y, Tan H, Hui X, Biomaterial scaffolds in regenerative therapy of the central nervous system, Biomed. Res. Int 2018 (2018), 10.1155/2018/7848901.

[41]. Hackett JM, Dang TT, Tsai EC, Cao X, Electrospun biocomposite polycaprolactone/collagen tubes as scaffolds for neural stem cell differentiation, Materials (Basel) (2010) 3714–3728.

[42]. Jaganathan J, Petit JH, Lazio BE, Singh SK, Chin LS, Tumor necrosis factor-related apoptosis-inducing ligand-mediated apoptosis in established and primary glioma cell lines, Neurosurg. Focus 13 (3) (2002).

[43]. Kim SM, Lim JY, Park SI, Jeong CH, Oh JH, Jeong M, Oh W, Park SH, Sung YC, Jeun SS, Gene therapy using TRAIL-secreting human umbilical cord blood-derived mesenchymal stem cells against intracranial glioma, Cancer Res. 68 (23) (2008) 9614–9623 Epub 2008/12/03 10.1158/0008-5472.can-08-0451. [PubMed: 19047138]

[44]. Reagan MR, Seib FP, McMillin DW, Sage EK, Mitsiades CS, Janes SM, Ghobrial IM, Kaplan DL, Stem cell implants for cancer therapy: TRAIL-expressing mesenchymal stem cells target cancer cells in situ, J. Breast Cancer 15 (3) (2012) 273–282 Epub 2012/10/24 10.4048/jbc.2012.15.3.273. [PubMed: 23091539]

[45]. Hingtgen S, Ren X, Terwilliger E, Classon M, Weissleder R, Shah K, Targeting multiple pathways in gliomas with stem cell and viral delivered S-TRAIL and Temozolomide, Mol. Cancer Ther 7 (11) (2008) 3575–3585, 10.1158/1535-7163.MCT-08-0640. [PubMed: 19001440]

[46]. Redjal N, Massachusetts General Hospital HMSMNaILBMU, Massachusetts General Hospital HMSDoRBMU, Massachusetts General Hospital HMSDoNBMU, Zhu Y, Massachusetts General Hospital HMSMNaILBMU, Massachusetts General Hospital HMSDoRBMU, Shah K, Massachusetts General Hospital HMSMNaILBMU, Massachusetts General Hospital HMSDoRBMU, Massachusetts General Hospital HMSDoNBMU, USA HUHSCICM,

Combination of systemic chemotherapy with local stem cell delivered S-TRAIL in resected brain tumors, Stem Cells 33 (1) (2017) 101–110, 10.1002/stem.1834.

[47]. Aboody KS, Najbauer J, Metz MZ, D'Apuzzo M, Gutova M, Annala AJ, Synold TW, Couture LA, Blanchard S, Moats RA, Garcia E, Aramburo S, Valenzuela VV, Frank RT, Barish ME, Brown CE, Kim SU, Badie B, Portnow J, Neural stem cell-mediated enzyme-prodrug therapy for glioma: pre-clinical studies, Sci. Transl. Med 5 (184) (2013), 10.1126/scitranslmed.3005365.

[48]. Hansen K, Muller FJ, Messing M, Zeigler F, Loring JF, Lamszus K, Westphal M, Schmidt NO, A 3-dimensional extracellular matrix as a delivery system for the transplantation of glioma-targeting neural stem/progenitor cells, Neuro-Oncology 12 (7) (2010) 645–654 Epub 2010/02/17 10.1093/neuonc/noq002. [PubMed: 20156807]

[49]. Bagó JR, Okolie O, Dumitru R, Ewend MG, Parker JS, Werff RV, Underhill TM, Schmid RS, Miller CR, Hingtgen SD, Tumor-homing cytotoxic human induced neural stem cells for cancer therapy, Sci. Transl. Med 9 (375) (2017), 10.1126/scitranslmed.aah6510.

[51]. Yan F, Li M, Zhang HQ, Li GL, Hua Y, Shen Y, Ji XM, Wu CJ, An H, Ren M, Collagen-chitosan scaffold impregnated with bone marrow mesenchymal stem cells for treatment of traumatic brain injury, Neural Regen. Res 14 (10) (2019) 1780–1786 Epub 2019/06/07 10.4103/1673-5374.257533. [PubMed: 31169196]

[52]. Huang G, Li F, Zhao X, Ma Y, Li Y, Lin M, Jin G, Lu TJ, Genin GM, Xu F, Functional and biomimetic materials for engineering of the three-dimensional cell microenvironment, Chem. Rev 117 (20) (2017) 12764–12850, 10.1021/acs.chemrev.7b00094. [PubMed: 28991456]

[53]. Sheets Kevin T., Ewend Matthew G., Mahsa Mohiti-Asli Stephen A. Tuin, Laboa Elizabeth G., Aboody Karen S., Hingtgen Shawn D., Developing Implantable Scaffolds to Enhance Neural Stem Cell Therapy for Post-Operative Glioblastoma, Molecular Therapy 28 (2020), 10.1016/j.ymthe.2020.02.008.

A

Scaffold	% CAC	Gelatin (% w/w)	Degradation Half-Life
Fast	46.0 ± 0.7	28.4 ± 1.97	0.8 ± 0.3 days
Slow	61.3 ± 1.7	29.0 ± 1.65	> 56 days

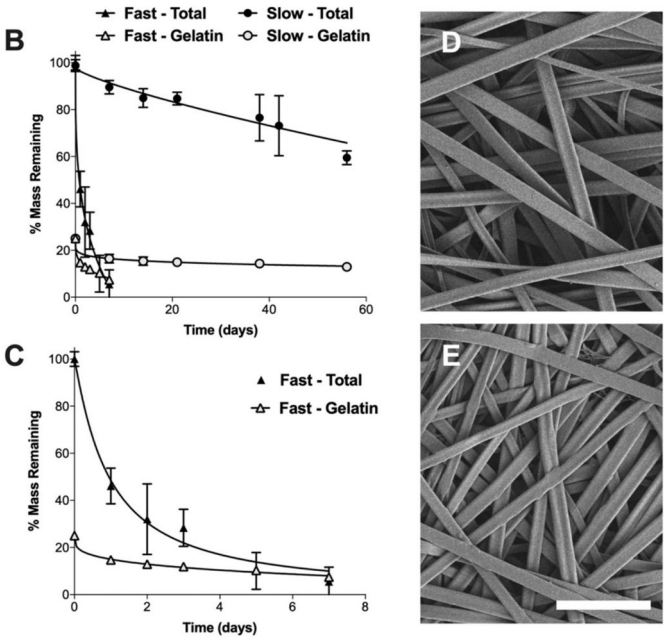

Fig. 1.

Degradation profiles of composite Ace-DEX gelatin scaffolds. (A) Table of fast and slow scaffold parameters, including Ace-DEX % cyclic acetal coverage (CAC), gelatin loading (% w/w), and degradation half-life of resulting scaffolds. (B) Degradation profiles of fast and slow scaffolds after 100 h of crosslinking. Percent of total scaffold mass (solid marker) and mass attributed to gelatin (open marker) are shown. (C) Fast degradation profile magnified. Data presented as mean ± standard deviation. Representative scanning electron microscopy (SEM) micrographs of scaffolds with (D) fast and (E) slow Ace-DEX gelatin scaffolds crosslinked for 100 h. Scale bar is 10 μm.

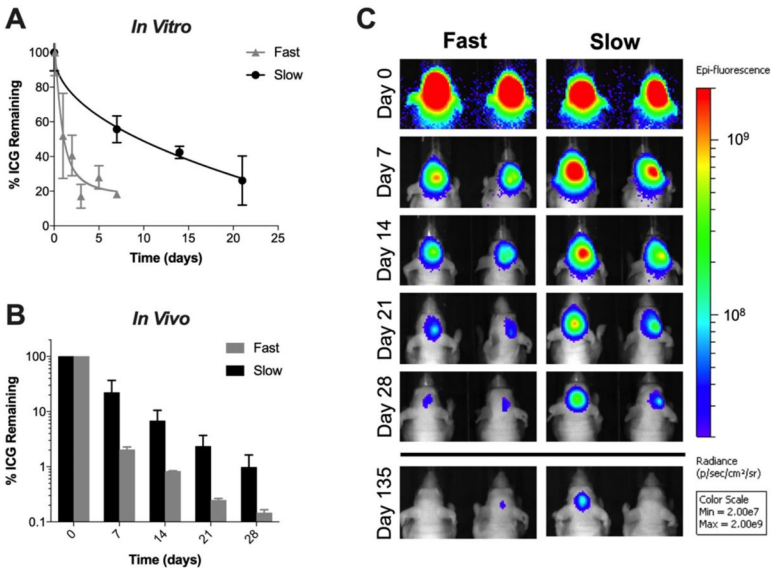

Fig. 2.

In Vitro and *Vivo* characterization of ICG-loaded Ace-DEX gelatin scaffolds. (A) *In vitro* characterization of ICG release from fast and slow Ace-DEX gelatin scaffolds. Data presented as mean ± standard deviation. (B) Quantified % remaining ICG at representative timepoints *in vivo*. Data presented as mean ± standard deviation. (C) Fluorescent images of ICG-loaded scaffolds impanated in the surgical resection cavity *in vivo* at representative time points. Fluorescence scale is in radiance (ρ/s/cm^2/sr) with limits set at 2.00×10^7 to 2.00×10^9 chosen to best visualize both the high initial signal and the disappearing signal thereafter.

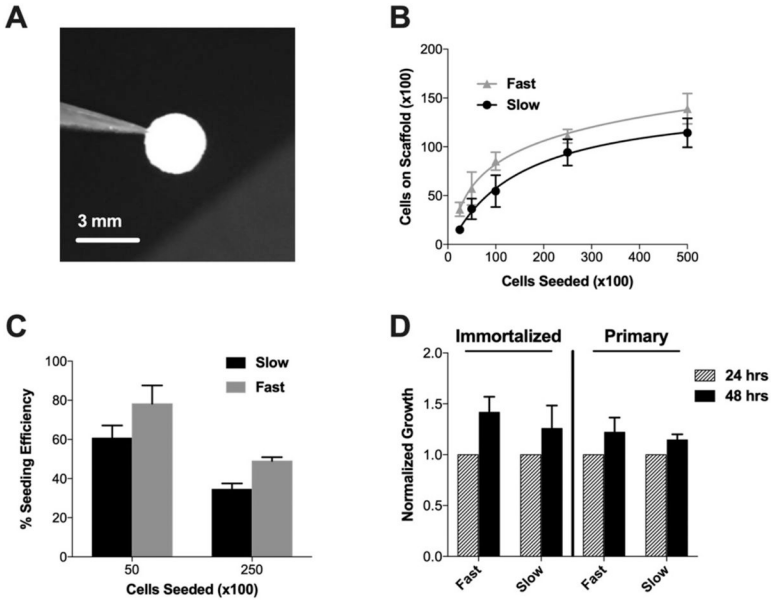

Fig. 3.

NSC seeding and viability on Ace-DEX gelatin scaffolds. (A) Image of 3 mm size scaffold scaled to fit in surgical resection cavity of a mouse. (B) Cell carrying capacity of scaffolds at 24 h with C17.2 NSCs. (C) Cell seeding efficacy determined by normalizing number of cells on scaffold to number of cells seeded for immortalized and primary NSCs. (D) Growth of cells seeded on scaffolds at 48 h, normalized to viability at 24 h for immortalized and primary NSCs. Data presented as mean ± standard error of the mean.

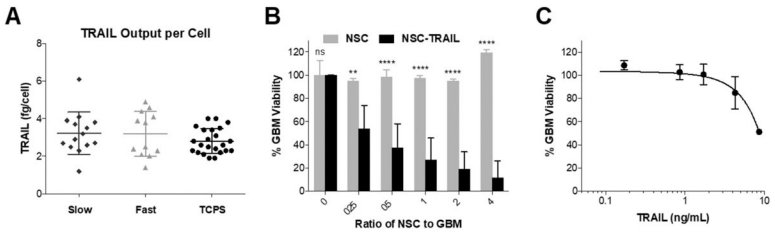

Fig. 4.

Generation of therapeutic NSCs and seeding onto scaffolds. (A) Quantification of TRAIL secreted from TRAIL-NSCs seeded onto fast and slow degrading scaffolds compared to TCPS. (B) Viability of GBM cells cultured with increasing ratios of unmodified NSCs or TRAIL-NSCs. (C) Viability of GBM cells treated with supernatant collected from NSCs containing secreted TRAIL. Data presented as mean ± standard deviation. ANOVA was done to determine statistical significance utilizing Tukey's multiple comparisons post-test. **P < 0.005 and ****P < 0.0001 with respect to NSCs of the same ratio to GBM.

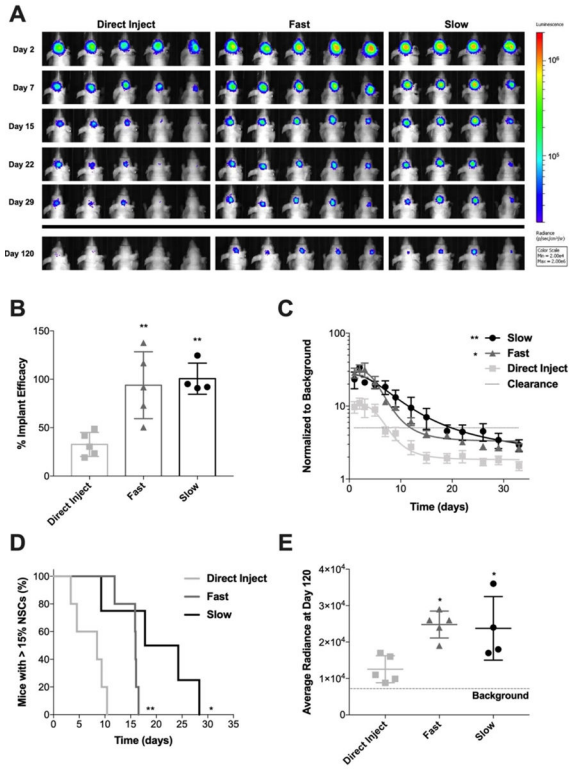

Fig. 5.

Persistence of NSC seeded on Ace-DEX gelatin scaffolds in resection cavity. (A) BLI images showing NSCs at representative time points after implantation in surgical resection cavity. BLI scale is in radiance (ρ/s/cm^2/sr) with limits set at 2×10^4 to 2×10^6. (B) Efficacy of NSC implant method comparing DI to NSC seeded on fast degrading and slow degrading scaffolds. Data presented as mean ± standard deviation. Statistical significance measured by ANOVA with Tukey's multiple comparison post-test. *P < 0.05 and **P < 0.005 with respect to DI. (C) BLI signal of NSCs in the brain normalized to background over time. Data presented as mean ± standard error of the mean. An ANOVA was done to determine significance of the AUC. **P < 0.005 with respect to DI. (D) Kaplan-Meier curve of NSC clearance from the brain comparing DI to NSCs seeded on fast and slow degrading scaffolds. Clearance was defined as BLI signal dropping below a 15% threshold. Log-rank (Mantel-Cox) test was done to determine statistical significance. *P < 0.05, **P < 0.005 with respect to DI. (E) Average radiance of NSCs at day 120 showing NSC implant efficiency. Data presented as mean ± standard deviation. Statistical significance measured by ANOVA with Tukey's multiple comparison post-test. *P < 0.05 with respect to DI.